



# Spatial and temporal variation of cooking-emitted particles in distinct zones using scanning mobility particle sizer and a network of low-cost sensors

Rubal Dhiman<sup>a</sup>, Rajat Sharma<sup>a</sup>, Akshat Jain<sup>a</sup>, Anirudha Ambekar<sup>a,b</sup>, Thaseem Thajudeen<sup>a,b,c,\*</sup>, Sarath K. Guttikunda<sup>d</sup>

<sup>a</sup> School of Mechanical Sciences, Indian Institute of Technology Goa, India

<sup>b</sup> Center of Excellence in Combustion Science, Indian Institute of Technology Goa, India

<sup>c</sup> Center of Excellence in Particulates, Colloids, and Interfaces, Indian Institute of Technology Goa, India

<sup>d</sup> TRIP-Centre, Indian Institute of Technology New Delhi, India

## ARTICLE INFO

### Keywords:

Indoor air quality  
Kitchen emissions  
Ultrafine particles  
Exposure duration  
Air exchange rate

## ABSTRACT

Exposure to ambient and household fine-particulate matter is identified as a substantial contributor to premature mortality in India, according to the Global Burden of Disease Studies. This study examines the impacts of typical Indian cooking practices on indoor air quality characteristics by monitoring the evolution of fine and ultrafine particle (UFP) concentration in the dining facility of a residential educational institute in India. The monitoring area was spread across the kitchen (zone 1) and the dining hall (zone 2). A combination of validated low-cost PM sensors (LCS), DustTrak8433, and Scanning Mobility Particle Sizer (SMPS) was utilized for real-time data acquisition while using Liquefied Petroleum Gas (LPG) as the cooking fuel. PM<sub>2.5</sub> and UFP concentrations were monitored at 1.3 m and 1.8 m from the floor to assess the vertical variation of pollutants during cooking activities, including breakfast, lunch, and dinner, and processes such as preheating, reheating, stir-frying, and deep-frying. It was found that the prolonged cooking durations involved in high-heat cooking methods like stir-frying and deep-frying resulted in a rise in coarser UFP (300–550 nm) and PM<sub>2.5</sub>, causing a higher exposure to PM and UFP concentration. PM<sub>2.5</sub> levels are higher at upper heights during typical cooking processes because of temperature-driven convection currents and hygroscopic growth of particles due to high humidity levels. Air exchange rates (AER) considerably varied by using chimneys and were low during the controlled (closed doors) compared to mixed ventilation (opened doors) conditions. The maximum AER was obtained during lunch (4.3–9.9 h<sup>-1</sup>) compared to breakfast (7.8–6.8 h<sup>-1</sup>) and dinner (0.55–7.9 h<sup>-1</sup>). The decrement rate of PM<sub>2.5</sub> inside zone 1 was highest during lunch (126 µgm<sup>-3</sup> h<sup>-1</sup>), coinciding with the highest AER during mixed ventilation. It is recommended that improving ventilation and better design of the kitchen can reduce the exposure of PM and UFP in commercial and rural area kitchens.

## 1. Introduction

A significant global impact on public health stems from indoor air pollution (IAP), underscored by J. Mu [1], and the widespread issue of indoor particulate matter (PM), particularly in developing countries, leads to 6.67 million annual fatalities, highlighting the need for individual exposure management. Among the different pollutants like PM, volatile organic compounds (VOCs), and polycyclic aromatic compounds (PAHs), the effect of PM stands out due to adverse impacts on air quality and human well-being [2,3]. The concentration of PM is classified according to their aerodynamic diameters, and classification typically includes 10 µm or less (PM<sub>10</sub>), 2.5 µm or less (PM<sub>2.5</sub>), 1.0 µm

or less (PM<sub>1</sub>), and 0.1 µm or less (PM<sub>0.1</sub>) is also known as UFP [4]. Over time, coarse particles (2.5 µm to 10 µm) can be trapped by nose hair or throat and dislodged through drinking water or other means [5]. Fine and UFP deeply infiltrate the respiratory system, contributing to coronary heart disease and premature mortality [6,7].

IAP, characterized by PM and UFP emissions, stems from diverse sources such as smoking, cooking, heating, and candle burning. A study states that cooking activities notably influence the indoor concentration of PM in households [8]. Investigation of the influence of cooking and post-cooking activities on IAP shows an increase in ultrafine concentration up to  $6 \times 10^6$  number/cm<sup>3</sup> [9]. 24-hour time-resolved measurements of PM<sub>2.5</sub> showed a median concentration of 79 µg/m<sup>3</sup>,

\* Correspondence to: Indian Institute of Technology Goa, Goa College of Engineering Campus, Farmagudi, Goa 403401, India.  
E-mail address: [thaseem@iitgoa.ac.in](mailto:thaseem@iitgoa.ac.in) (T. Thajudeen).

mainly due to cooking-related emissions [10]. These findings underscore the dynamic nature of emissions and indoor concentrations of cooking-related PM, both in terms of number concentration (NC) and mass concentration (MC) [11]. Several studies have characterized the indoor levels of various gases like  $\text{NO}_x$ ,  $\text{SO}_x$ , and coarser PM generated during cooking fueled by natural gas and using Chinese cooking methods [1,8,12,13]. A few studies have been done to study the impact of various Indian cooking stove types on fine PM and UFP concentrations [3,13,14]. For further details, please refer to Table S3a and b (Supplementary Information) for additional information on relevant studies related to emissions from cooking stoves. Very few studies exist on how indoor PM and UFP concentration levels vary from diverse Indian cooking processes and activities [13,15].

Crucial factors contributing to cooking emissions include the selection of cooking oils, cooking duration, fuel type, ingredients, cooking temperature, cooking method, and ventilation conditions [12,16]. While some studies have explored some of these influential factors [3,17,18], there remains a need for a comprehensive assessment of how all these variables collectively impact IAQ in Indian cooking environments. Reference grade instruments, including GRIMM EDM 264 and aerodynamic particle sizer, are used for monitoring PM concentration from cooking processes [19,20], while LCS has been used for monitoring the PM and gas species to establish a relation among these factors [2,3]. Concerns over the accuracy of LCS can be addressed by adequately calibrating it by collocating it to the reference grade equipment [21,22]. By expanding the deployment of LCS, a more comprehensive network for monitoring can be realized, which enhances the capabilities to access air quality variations [23–25].

A detailed understanding of the air quality levels away from the sources requires a network of LCS devices. Along with the distance from the sources, fluctuations along the vertical directions are also relevant due to the strong convection current caused by cooking activities [26,27]. This is essential to identify the requirements for effective ventilation to minimize exposure [3,17,28–30]. The air exchange rate (AER) impacts how pollutants flow from indoors to outside during ventilation. For instance, opening windows can boost AER by as much as  $2 \text{ h}^{-1}$ , while fans can increase AER by up to  $1 \text{ h}^{-1}$  [31]. Optimizing the AER reduces the accumulation of fine and UFP, leading to better IAQ. Additionally, some cooking emission studies near the source offer insights into household exposure [2,10,15,32]. However, it is crucial to measure PM and UFP far from cooking sources to assess total indoor air quality (IAQ) [17,30] and comprehend pollutant dispersion [9]. Notably, the concentration levels of fine particulate matter ( $\text{PM}_{2.5}$ ) were observed to decrease with prolonged heating, while the concentration of coarser particles ( $\text{PM}_{10}$ ) increased due to coagulation effects [33].

Our understanding of the effect of cooking activities and duration on the fine PM and UFP emissions remains limited. To address this gap, it is critical to thoroughly understand the features of fine PM and UFP emissions during the cooking process, like preheating, reheating, stir-frying, and deep-frying, and evaluate exposure patterns and risk assessment for kitchen workers. Although several prior studies have focused on cooking emissions, the assessment of IAQ with vertical profiling based on height variation for UFP and fine particles has not been done for different cooking processes. The influence of environmental parameters like temperature and relative humidity (RH) on different cooking activities like breakfast, lunch, and dinner must also be examined. Existing research has predominantly emphasized sensor-based measurements of cooking emissions. However, a significant knowledge gap exists regarding the strategic utilization of LCS for assessing the exposure to PM concentrations among different individuals and for evaluating ventilation patterns, including the determination of AER. The concerns in LCS related to accuracy are mitigated through rigorous calibration and systematic evaluation of bias correction against the reference monitor. This study also aims to optimize IAQ assessment in kitchen and dining areas by strategically deploying a network of PM sensors at key locations. For this investigation, zone 1 (kitchen) and

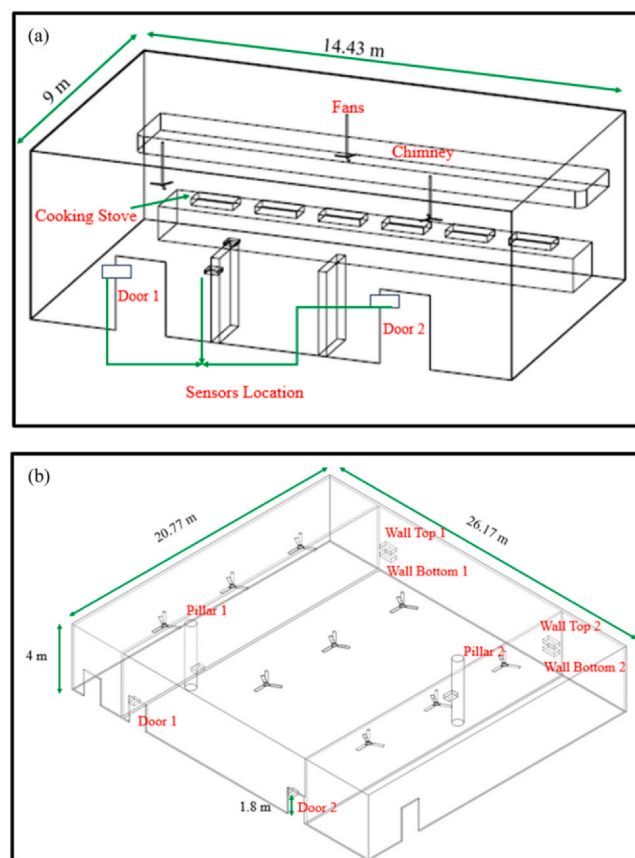


Fig. 1. Schematic Layout of (a) Zone 1 (Kitchen) and (b) Zone 2 (Dining hall).

zone 2 (dining area) have been selected for analysis. Kitchen (zone 1) is equipped with specific ventilation sources, a chimney, and two open interfaces serving as shared entry points, while the dining hall (zone 2) is the dining area. The overarching goal is to identify potential biases based on exposure methodology and evaluate critical parameters such as sensor placement, AER, background concentrations, decay rates, and exposure indices.

## 2. Methodology

### 2.1. Study area

The experimental study was conducted in the kitchen (zone 1) and dining (zone 2) areas at a residential educational campus in India. Fig. 1 depicts the schematic model for the experimental study area consisting of zone 1 and zone 2 with an area of  $99.94 \text{ m}^2$  and  $210 \text{ m}^2$ , respectively. Zone 1 has specific ventilation sources (chimney) and two open interfaces  $1.5 \times 2.1 \text{ m}^2$ , which serve as common entry points between zone 1 and zone 2. The mechanical ventilation fan was initiated at the start of the breakfast activity (0–240 minutes) preparation and ran without interruption until the conclusion of the lunch activity (0–240 minutes), spanning approximately 8 hours. After a brief pause, mechanical ventilation resumed before the start of the dinner activity and operated until 180 minutes into it, aligning with the completion of the dinner activity. No further activity was planned for the remainder of the day, and the next ventilation cycle was scheduled for the following morning. After the completion of the dinner activity, the no-activity period is known as the settlement period in our study. Additionally, there are three ceiling fans positioned at a height of 3 m and a distance of 0.5 m from each other. The gas stoves are located at a distance of 5.5 m from the interface. In zone 2, the dining area, with 60 tables and 25 ceiling fans, has a seating capacity of 600 individuals. For this

research, the sensor placement in zone 2 encompasses 53.33% of the total seating capacity. The measurement period spanned 54 days, from May 2023 to July 2023, during which the food menu and the quantity of food prepared remained consistent, catering to the usual number of individuals during regular activity periods. The advantage of such a facility is consistency in the menu. Food at the facility is prepared exclusively using Liquefied Petroleum Gas (LPG) as fuel for the cooking stoves.

## 2.2. Data collection and experimental setup

UFP concentrations were measured using the TSI Scanning Mobility Particle Sizer (SMPS) Electrostatic classifier, Model 3082, and PM concentration was measured using TSI Dusttrak DRX Aerosol Monitor 8533 (DT) and LCS network. The LCS used in this study are PMS 5003 and PMS 7003 offer high-resolution data through light scattering [34]. The study centered on the usage of LCS and DT to measure PM<sub>2.5</sub> MC in zone 1, while SMPS assessed total number concentration (TNC) and size distribution within the 15 nm to 550 nm range. Continuous calibration with DT was carried out after deploying PMS 5003 and PMS 7003 to ensure PM measurement accuracy. As shown in Fig. 1, the measurement points were positioned at heights of 1.3 m and 1.9 m to cover the typical breathing zone. These selected monitoring points were intended to offer insight into PM and UFP distribution within the specified zone of interest for different cooking activities and processes. Sensors were also strategically positioned at a distance from the cooking source to capture the comprehensive behavior of PM and UFP when they were not in close proximity to the emission sources. PM<sub>2.5</sub> and UFP concentrations were analyzed across different cooking activities like breakfast, lunch, and dinner and during different cooking processes like preheating, stirring, reheating, and deep frying. A comprehensive survey was devised and carried out in zone 1 for analysis, focusing on factors such as the duration of cooking activities, the diversity of cooking processes that vary with time, and variations in the use of cooking oil. The experimental setup was established in zone 1, where the period of cooking activities was recorded, and workers were surveyed regarding the oil usage during each process and activity. Controlled ventilation was achieved by utilizing a chimney extractor located in zone 1, which remained operational throughout the measurement campaign. Kitchen emissions were closely monitored in a cutting-edge educational facility, with non-cooking activities like cleaning and maintenance scheduled at specific times to minimize their impact. Dust resuspension was addressed by cleaning zone 1 after each activity.

Within zone 2, sensors were strategically positioned at six distinct locations, all at breathing height. These sensor placements collectively covered 53.33% of the seating capacity. Notably, pillar 1 and pillar 2 were specifically chosen due to their positioning in front of doors through which PM and UFP migrated from zone 1 to zone 2. These selected locations served as key points for capturing a significant portion of PM for measurement purposes. The sensors mounted on the walls in zone 2 primarily aimed to measure PM that traveled farthest from the emission sources. The primary objective of monitoring in zone 2 was to assess the extent of commuters' exposure to cooking-related emissions.

## 2.3. Data analysis

### a) Sensors design

Plantower PMS 5003 and PMS 7003, used for measuring PM<sub>2.5</sub> and equipped with Arduino UNO R3 boards, were used for the study, where the sensors collected and stored data, including date and time stamps, on memory cards. A BME 280 sensor paired with Arduino was also used to measure temperature and humidity. Each equipment unit is priced at approximately 5000 Indian Rupees (approximately 60 USD). The low-cost PM sensors measured PM<sub>1</sub>, PM<sub>2.5</sub>, and PM<sub>10</sub> concentrations (µg/m<sup>3</sup>) every second. PMS 5003 sensor has been shown to exhibit a strong

correlation with the gravimetric method, as demonstrated by A. Masic [35], while with beta attenuation monitor, PMS 5003 shows a coefficient of determination (R<sup>2</sup>) of 0.53, as reported by C. McFarlane [36]. Correlation analyses have been conducted on these LCS alongside the DustTrak 8433 TSI instrument for over two months to assess their consistency. Furthermore, they were co-located for fifteen days to evaluate the inter variability of LCS. Inter-variability refers to determining the consistency of measurement between the two sensors when two sensors are subjected to the same environmental conditions.

## 2.4. Airflow characterization methodologies

### a) Air Exchange Estimation

The tracer gas method, as outlined in [37], involves the application of a mass balance approach within a confined space. CO<sub>2</sub> is typically used for estimating AER with the tracer gas method, and in this study, CO<sub>2</sub> concentration was measured using three Winsen MH Z19C sensors. The method formulates that the mass balance of tracer gas can be expressed inside a single space, as shown in Eq. 1.

$$V \frac{dC(t)}{dt} + Q_{Zone,exhaust} C_{out} - Q_{Zone,Supply} C(t) + S = 0 \quad (1)$$

where  $V$  (m<sup>3</sup>) is the volume of the space,  $C(t)$  is the concentration of CO<sub>2</sub> gas at instant  $t$ ,  $t$  (s) is time,  $S$  is the generation rate of the tracer gas,  $Q_{Zone,exhaust}$ ,  $Q_{Zone,Supply}$  is the external and internal exchange rate,  $C_{out}$  is the external concentration of tracer gas.

The analytical solution of Eq. 1 is given by Eq. 2.

$$\ln \left[ \frac{C_{Zone,in,t} - \bar{C}_{out}}{C_{Zone,in,t=0} - \bar{C}_{out}} \right] \times \frac{1}{\Delta t} = -AER \quad (2)$$

where  $\bar{C}_{out}$  is the mean outdoor concentration,  $C_{Zone,in,t}$  is the CO<sub>2</sub> concentration inside zone at time  $t$ ,  $C_{Zone,in,t=0}$  is the CO<sub>2</sub> concentration at the inside zone at the start.

The AER was determined using CO<sub>2</sub> concentration from three sensors—two in zone 2 and one in zone 1. The sensor positioned near door 1 in zone 2 is responsible for measuring the CO<sub>2</sub> concentration (inside zone 2), as it serves as one of the points through which air enters zone 1. In zone 1, the recorded CO<sub>2</sub> concentration values encompass emissions from activities such as cooking or individual contributions. CO<sub>2</sub> measurements were conducted every minute during the measurement campaign in both zone 1 and zone 2. The density difference between the air and CO<sub>2</sub> is significantly lower compared to solid particles [4], making CO<sub>2</sub> more prone to dispersion in the air and ensuring uniform mixing within zone 1. Additionally, the continuous functioning of three fans (zone 1) during different activities contributes to providing uniform mixing for CO<sub>2</sub>. Furthermore, the chimney acts as a ventilation fan (zone 1), facilitates air circulation, and helps evenly distribute CO<sub>2</sub> inside zone 1. Two CO<sub>2</sub> sensors were strategically placed at a 7 m distance from each other to assess the variation in CO<sub>2</sub> concentration within the zone 1. The results indicate a slope approaching 1, signifying consistent readings between sensors at different points in zone 1 and suggesting uniform mixing of CO<sub>2</sub>. With an overall percentage difference of 9% during breakfast, lunch, and dinner activities, it is reasonable to infer that the area demonstrates a uniform mixing of CO<sub>2</sub>. The AER was evaluated during different cooking processes, activities, and ventilation scenarios of mechanical (only the chimney is operational and doors are closed) and mixed systems (chimney and doors are opened).

### b) Decay rate analysis

The decay rate refers to the rate at which pollutants decrease in quantity over a period of time following their release [38]. The decay rate analysis was performed based on zonal division. The difference between PM concentration at the initial and final time with respect to the total duration of activity provides a decay rate [3]. The decay rate measured for each activity performed during the day depends on the

AER. Average  $PM_{2.5}$  decay can be calculated by using Eq. 3, where  $t_a$  is the time duration of the activity,  $PM_{2.5}^0$ , and  $PM_{2.5}^t$  are  $PM_{2.5}$  concentrations during the initial and final phase of the cooking activity for mechanical and mixed ventilation.

$$\text{Decay Rate} = \frac{PM_{2.5}^0 - PM_{2.5}^t}{t_a} \quad (3)$$

### 2.5. Exposure-based relative bias analysis and assessment of exposure risk

The relative bias was obtained between  $PM_{2.5}$  concentration measured from DT and LCS inside zone 1, based on the exposure analysis during different cooking activities. The background concentration ( $C_{BG}$ ), or the environmental settlement value, is removed from the  $PM_{2.5}$  concentration to identify the exposure from the sources of zone 1. Details can be seen in the SI document S1.1. The USEPA [39] provides a detailed method for calculating the exposure risk in term of potential inhaled dose ( $I_{dose}$ ) from intake procedures such as inhalation. The details on the exposure to health risks are shown in section S1.2.

## 3. Results and discussion

### 3.1. Cooking processes and emission characteristics

$PM_{2.5}$  and UFP concentrations were analyzed across different cooking activities like breakfast, lunch, and dinner and during different cooking processes like preheating, stir-frying, reheating, and deep frying at different heights are compared. For comparison of UFP emissions, size ranges from 15–550 nm were divided into 15 size bins, and the NC of particles in each of the bins were calculated from SMPS measurements. TNC refers to overall particle concentration across a defined size range of 15–550 nm, and NC refers to the concentration of particles within a specific size bin. We initially categorized the data into 15 bins for visualization in the graphs for SMPS; however, for enhanced clarity and precision in our explanation, we further subdivided these 15-size categories into three groups: UFP (15–100 nm), fine particles (100–300 nm), and coarser UFP (above 300 nm). The  $PM_{2.5}$  concentration from PMS 5003 for different cooking processes and activities was calibrated with DT inside the zone 1 and details of calibration is shown in Fig. S1. The coefficient of determination (COD) values for different sensors during this period exceeded 0.72, indicating a strong correlation to DT measurements. Intra-sensor comparisons for PMS 5003 showed strong COD ( $R^2 = 0.98\text{--}0.99$ ) among the sensors, and the slope among all sensors was close to one, as shown in Fig. S2. COD between LCS and DT fell within the range reported in laboratory and ambient studies, but the PMS5003 and Winsen sensors underestimated  $PM_{2.5}$  concentrations compared to DT, consistent with prior studies [40,41]. The variation of  $PM_{2.5}$  with different climatic background parameters measured with BME 280 can be seen from Fig. S3. A Pearson correlation test was performed to identify the relationship between meteorological parameters inside zone 1 and  $PM_{2.5}$ . The environmental parameters like humidity temperature were analyzed with  $PM_{2.5}$ . The detailed analysis of the environmental factors variation is discussed in detail in S1.4.

Preheating oil during breakfast activity is typically less than 8 minutes, which is shorter than lunch and dinner activity. This discrepancy can be attributed to the varying quantity of oil used, as shown in Table S4. Table 1 shows that  $PM_{2.5}$  emissions were more pronounced during the stir-frying phase when compared with the preheating process. This can be due to the higher temperature resulting in the degradation and evaporation of cooking oil, releasing compounds responsible for PM emissions. The more prolonged exposure during the stir-fry process allows more substances in food, such as oil or fats, to vaporize and produce emissions [42]. Stir-frying with constant stirring or flipping of the food leads to faster cooking and increased emissions compared to a passive preheating process Fig. 2.

Fig. S4, S5, and S6 represent the day-wise average PM concentration variation during breakfast, lunch, and dinner activity, respectively, for preheating and stir-frying at upper and lower heights. The percentage change after 5 minutes in Figs. 3 and 4 signifies the variation since the beginning of the process, while the percentage change after 10 minutes denotes the shift in values between the 5-minute mark and the 10-minute mark; similarly, the percentage change after 15 minutes signifies the shift in values between the 10 minutes mark to 15 minutes mark, and this pattern continues. The chimney and interface doors are the only ventilation modes. The minimum average background concentration for  $PM_{2.5}$  was  $28 \mu\text{g}/\text{m}^3$ .

#### a) Fine PM and UFP emissions from the preheating process

The results from Figs. 2–4 and Tables 1 and 2 also suggest that during preheating for breakfast, lunch, and dinner activities:

- $PM_{2.5}$  and TNC are higher at lower heights during breakfast (Fig. 2a and d) (Tables 1 and 2), possibly due to the lower temperature ( $33 \pm 1 \text{ }^\circ\text{C}$ ) and RH ( $61 \pm 4\%$ ) earlier in the day compared to temperature ( $35 \pm 2 \text{ }^\circ\text{C}$ ) and RH ( $64 \pm 8\%$ ) during the rest of the day. This leads to particles being situated at a lower height, resulting in higher concentrations.
- For NC, UFP (15–100 nm), especially 15–50 nm and fine particles (100–300 nm), initially exhibits a higher presence at an upper height (Fig. 4a) during the initial preheating phase for breakfast, leading to the lower PM concentration at upper height during the start of breakfast activity.
- The coarser particles (above 300 nm) were more at lower height (Fig. 3a) during the initial preheating phase for breakfast, causing the higher PM concentration at lower height, leading to a higher PM concentration at lower height during the start of breakfast activity.
- $PM_{2.5}$  and TNC are higher at upper heights during lunch (Fig. 2b and e) and dinner (Fig. 2c and f) activities, possibly due to higher temperatures ( $33\text{--}37 \text{ }^\circ\text{C}$ ); particles begin to ascend, resulting in more particles of different sizes at upper heights, leading to higher concentrations (Tables 1 and 2).
- The NC variation across the different size bins shows the higher presence of UFP, fine, and coarser UFP at upper height during lunch (Fig. 4b) and dinner (Fig. 4c) activity from the beginning of preheating to its end. This results in more  $PM_{2.5}$  concentration at upper height from beginning to end, as shown in Figs. 3 and 4. The behavior between  $PM_{2.5}$  and TNC shows directly proportionality.
- As the preheating process continues, there is an increment in coarser size particles at upper height, causing an increase in  $PM_{2.5}$  concentrations during all activities.

#### b) Fine PM and UFP emissions from the stir fry process

The results from Figs. 2–4 and Tables 1 and 2 also suggest that during stir-frying for breakfast, lunch, and dinner activities:

- The  $PM_{2.5}$  concentrations were higher at the upper height (Tables 1 and 2) during all activities, possibly because of higher temperatures ( $2\text{--}5 \text{ }^\circ\text{C}$  more) after preheating during all activities, causing the particles to move upward.
- Increased RH (22%) can lead to particle size enlargement, contributing to higher  $PM_{2.5}$  concentrations at upper heights leading to higher  $PM_{2.5}$  concentration.
- The TNC during this process was higher at a lower height for all activities, contrasting with  $PM_{2.5}$  concentration, likely due to the dominance of larger particles. This tells us that the larger particle size, even having less NC, still contributes more to the PM concentration than the smaller particles having more NC.
- The NC variation for the stir-frying process shows increased coarser-sized particles at upper heights, leading to elevated PM concentrations at the end of the preheating process during breakfast activity.
- During breakfast, as the stir-frying process proceeds, there is an increase in the concentration of coarser particles at upper height, noticeable from 10 to 20 minutes of the process, as shown in Fig. 4a.

**Table 1**  
PM<sub>2.5</sub> (µg/m<sup>3</sup>) emission during different cooking processes and activities.

Activity	Processes	Lower Height				Upper Height			
		Average	SD	Minimum	Maximum	Average	SD	Minimum	Maximum
Breakfast	Preheating	154	68	81	189	115	32	38	149
	Stir Fry	170	54	147	198	238	123	157	283
Lunch	Preheating	124	26	84	199	166	20	26	252
	Stir Fry	291	48	228	317	304	46	243	352
	Reheat	311	146	205	401	415	14	162	500
	DeepFry	414	147	359	464	437	121	320	566
Dinner	Preheating	110	47	69	153	158	48	29	256
	Stir Fry	131	44	112	157	240	86	206	299
	Reheat	355	71	131	604	663	30	274	856
	DeepFry	503	153	369	719	632	67	535	813

- During lunch, there is a slight decrease in coarser particles at the upper height after 10 minutes (Fig. 3b and 4b). This led to a drop in PM concentration at the upper height and a higher PM concentration at the lower height (Fig. 2b). This pattern could be attributed to the practice of covering cooking utensils in between the cooking process.
- Subsequently, there was a rise in coarser particles at upper height, leading to higher PM concentration. During dinner, there was a continuous rise in NC of coarser particles till the end of stir fry activity at upper height, leading to higher concentration throughout the process.
- Coarser particles rise at the lower height compared to the upper height as dinner activity concludes, notably during the final stages of stir-frying (Figs. 3c and 4c). This shift is likely due to higher humidity levels, resulting in particle deposition at the lower height.

### c) Fine PM and UFP emissions from the Reheating and deep fry processes

After the preheat and stir fry processes, the reheating process occurs on specific days, and typically, interface doors are kept open. Breakfast does not involve any reheating and deep fry process. The deep frying process typically starts after 12 minutes of reheating. During reheating and deep frying, hotter oil leads to the breakdown of oil particles, resulting in higher PM and UFP emissions than in stir-fry and preheating processes. The repeated heating of oil during the deep fry process potentially leads to chemical reactions within the oil. These reactions can release VOCs, which ultimately contribute to the formation of UFP or PM when they come into contact with oxygen in the air [42]. The other reason for higher emissions during the reheating of oil is the food residues left in the oil from the previous cooking activities. These residues will break down and contribute to the formation of PM and UFP [12]. The comparison of the reheat and deep fry process for upper and lower heights for lunch and dinner on different days in a week is shown in Fig. S7.

The results from Figs. 5, 6, S8, S9, and Tables 1 and 2 also suggest that during reheating and deep-frying for lunch and dinner activities:

- The PM<sub>2.5</sub> concentration during these processes is higher at upper height during lunch and dinner (Fig. 5a and b). An increase in temperature (35–37 °C) causes particles to ascend to the upper height, and an increase in RH (16% increase) can enlarge these particles.
- The TNC is more at a lower height during reheating and deep fry activities, indicating an increase in PM concentration even when there is a decrease in TNC during lunch. This is because of the dominance of the bigger particles.
- The fluctuation in particle NC across various sizes during lunch activity suggests that during the initial phases of reheating, smaller UFP up to 100 nm are more prevalent at lower height, while larger

particles dominate the NC at upper height, leading to higher PM<sub>2.5</sub> at upper height.

- As the reheating process ends, coarser particles are present at the upper height during lunch activity, causing more increase in PM<sub>2.5</sub> there. When deep frying commenced, there was an observed increase in the NC of coarser particles at upper height, around the 15-minute mark (Fig. S8b). Around the 25-minute point, a noticeable reduction in coarser particles at upper height is evident, leading to a decrease in PM concentration (Fig. 5a).
- Similarly, at approximately 35 minutes (Fig S8b), there is a decline in UFP, fine and coarser particles at upper height, leading to a drop in PM<sub>2.5</sub> concentration (Fig. 5a).
- After that, there is again a rise in PM<sub>2.5</sub> concentration at upper height near 40 minutes of processes because of increased coarser size particles. Towards the end of the lunch activity, there was a decrease in all size particles at upper height because of higher RH, causing the particles to settle and reducing PM<sub>2.5</sub> concentration.
- As depicted in Fig. 5, there is a noticeable decline in PM<sub>2.5</sub> concentration during lunch activity around the 12-minute mark, followed by a subsequent increase. This transition corresponds to the conclusion of the oil reheating phase and the commencement of deep frying activity.
- The fluctuation in concentration of PM<sub>2.5</sub>, TNC, and NC of different sizes after the initiation of deep frying is due to the changing demand for food, which depends on the number of individuals present within zone 2. More people in zone 2 trigger the deep frying process, which raises emissions, whereas fewer individuals result in a reduced deep frying process and, consequently, lower emissions.
- Towards the end of the lunch activity, the RH peaks, leading to particle enlargement and subsequent settling of particles. This results in an increase in both TNC and NC across various particle sizes at the lower height.
- At the beginning of the reheating during the dinner activity, PM<sub>2.5</sub> was higher at the upper height, and TNC was higher at the lower height. However, as the activity progresses, the TNC increases at upper height, consistent with the pattern observed during deep frying activity.
- This behavior is attributed to the TNC of UFP during different intervals, as shown in Fig. 5c and d. The TNC during the starting process of reheating for dinner was higher at the upper height for UFP, fine, and coarser UFP, which caused the sudden increase in PM concentration.
- Towards the end of the reheating process and the beginning of the deep frying process, approximately at the 12-minute mark, there is an observed decrease of coarser particles at upper height (Fig. S9a and b), resulting in a reduction of PM concentration. As the deep frying process continues, there is a subsequent increase in the concentration of these larger particles, leading to a rise in PM<sub>2.5</sub> concentration.

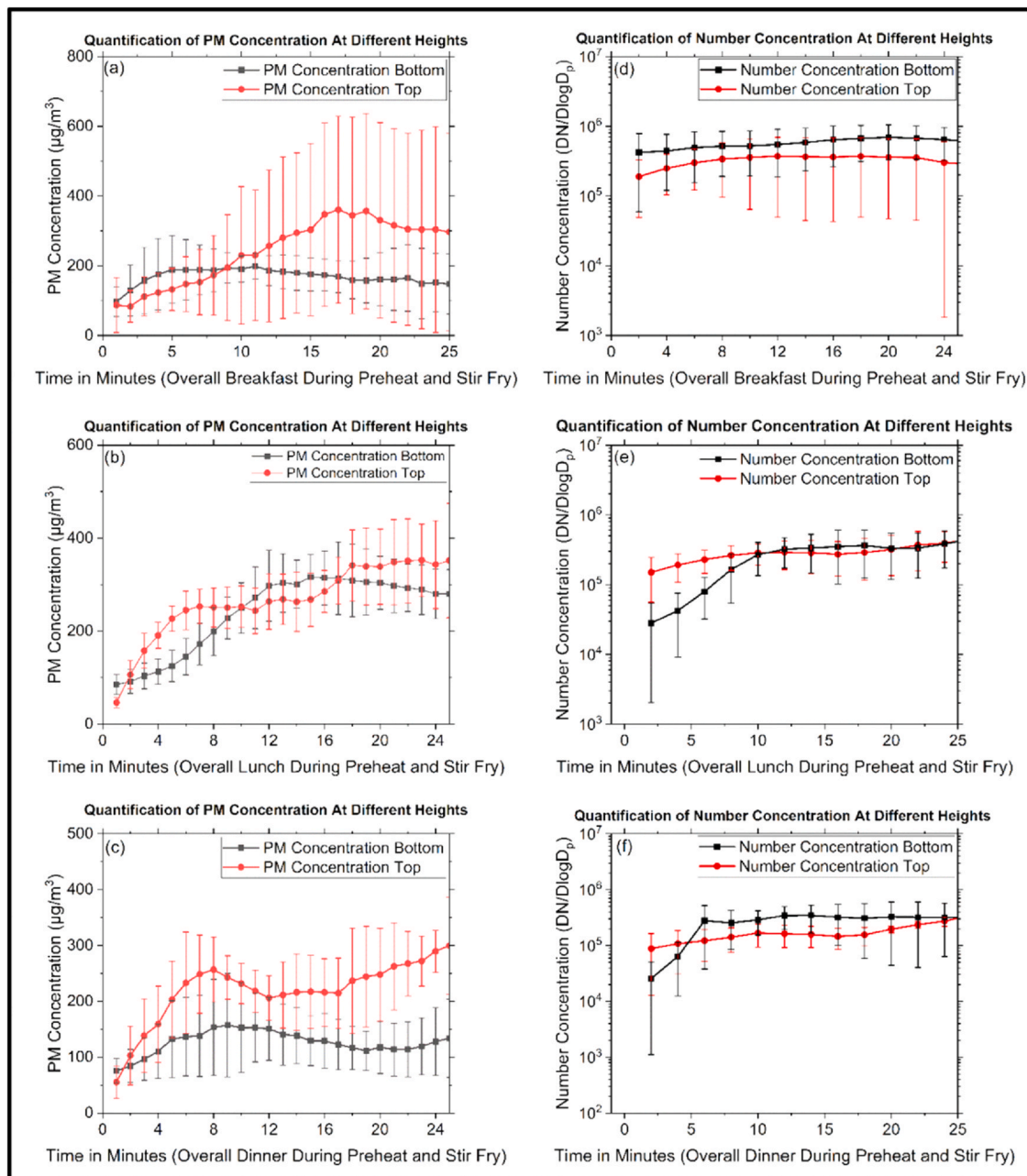


Fig. 2. Comparison of (a)  $\text{PM}_{2.5}$  for breakfast, (b)  $\text{PM}_{2.5}$  for lunch, (c)  $\text{PM}_{2.5}$  for dinner, (d) TNC for breakfast, (e) TNC for Lunch, and (f) TNC for dinner for preheat and stir-frying measured by LCS at two different heights. The x-axis measures elapsed time in minutes from the start of cooking, while the y-axis displays concentration levels at specific time intervals. Error bars represent the standard deviation among the data observed across multiple weeks.

### 3.2. Analyzing concentration-based airflow characterization parameters

#### a) Zonal airflow estimation

Zone 1 has controlled ventilation through the chimney with a 5030 CFM flow rate for an area of  $390 \text{ m}^2$ , i.e., zone 1. During the first hour of activity, the chimney is operational with the interface door closed, which makes zone 1 a controlled environment with the possibility of leakage through infiltration from the gaps between interface doors. The ACH (air change per hour) from the chimney while working in a controlled environment is  $12.8 \text{ h}^{-1}$ . After opening the interface door, the flow will be from zone 2 to zone 1 because of the chimney.

The settlement zone shows an AER range of  $-1.08 \text{ h}^{-1}$  to  $-4.74 \text{ h}^{-1}$ , and negative values indicate that the airflow is from zone 1 to zone 2 during the settlement period. Positive AER values suggest airflow from zone 2 to zone 1, possibly due to mechanical ventilation,

whereas negative AER values indicate airflow from zone 1 to zone 2, likely resulting from the lack of mechanical ventilation. Another factor contributing to the flow from zone 1 to zone 2 in the absence of mechanical ventilation is the closed nature of zone 1, creating higher pressure compared to zone 2, thereby causing the airflow from zone 1 to zone 2. During the breakfast activity in the controlled ventilation, the AER lies between  $0.52$  and  $2.65 \text{ h}^{-1}$  from a single interface, as shown in Fig. 6a. The AER variation during mixed ventilation lies between  $1.1$  and  $6.8 \text{ h}^{-1}$ . The AER rate for the initial preheating of breakfast and stir fry phase is less during controlled ventilation than mixed ventilation, in which the interface doors are also opened. The low AER rate during breakfast activity can cause higher UFP concentration during the first 10 minutes of cooking, where the NC of particle size up to  $100 \text{ nm}$  dominates. However, as the cooking process progresses, there is an increase in RH and a shift towards larger particles, specifically more

**Breakfast: Preheat and Stirfry (Lower Height)** (a)

Particle Size	NC	% C (5 Min)	% C (10 Min)	% C (15 Min)	% C (20 Min)	% C (25 Min)
15 to 20	6,731	1,798	4,893	-42.3	-1.7	-26.6
20 to 25	38,423	772	3,493	1.3	-51.1	-34.0
25 to 30	8,551	700	21,275	-3.9	-23.5	-40.3
30 to 40	14,621	632	-3,241	32.2	-7.1	-5.6
40 to 50	9,840	397	-1,199	92.9	23.6	-18.3
50 to 60	6,922	196	-542	128.0	51.9	-12.9
60 to 80	8,137	89	-147	156.9	64.8	-1.3
80 to 100	4,375	56	23	188.8	54.5	12.5
100 to 140	3,735	40	103	208.3	38.1	-2.9
140 to 180	1,248	39	79	281.1	33.8	16.8
180 to 220	540	41	45	344.0	28.7	1.8
220 to 300	401	54	82	-70.4	34.7	289.3
300 to 380	272	-39	188	-161.8	41.8	40.7
380 to 460	187	-27	1,065	205.2	74.9	104.8
460 to 520	33	144	164	664.8	70.4	-3.0

**Lunch: Preheat and Stir fry (Lower Height)** (b)

Particle Size	NC	% C (5 Min)	% C (10 Min)	% C (15 Min)	% C (20 Min)	% C (25 Min)
15 to 20	5,576	120.9	1,235	183.6	13.0	1.74
20 to 25	40,897	173.1	1,553	300.8	25.5	-3.92
25 to 30	6,062	175.4	1,202	367.3	30.3	-2.97
30 to 40	11,234	77.9	695	431.4	59.1	-2.76
40 to 50	8,836	33.5	525	357.0	96.3	5.02
50 to 60	6,564	11.4	443	230.0	133.1	12.29
60 to 80	6,277	-1.9	364	158.7	156.0	16.29
80 to 100	2,667	-0.4	323	124.7	154.6	17.44
100 to 140	1,655	1.9	319	104.5	155.1	12.30
140 to 180	580	13.8	264	111.5	163.2	3.51
180 to 220	252	38.2	321	130.4	142.0	1.40
220 to 300	191	68.2	332	151.9	103.9	-2.38
300 to 380	71	109.8	304	280.3	46.9	15.93
380 to 460	21	319.6	248	347.6	15.4	24.46
460 to 520	20	115.6	358	345.5	13.9	11.58

**Dinner: Preheat and Stir Fry (Lower Height)** (c)

Particle Size	NC	% C (5 Min)	% C (10 Min)	% C (15 Min)	% C (20 Min)	% C (25 Min)
15 to 20	1,189	1,772	88	25.5	-3.8	30.7
20 to 25	6,614	1,628	509	44.3	18.2	32.5
25 to 30	950	2,121	825	67.9	15.5	52.2
30 to 40	1,621	1,385	1,121	83.6	25.5	71.4
40 to 50	1,536	839	835	127.8	20.7	91.2
50 to 60	1,546	510	636	132.7	22.4	82.6
60 to 80	2,346	339	659	113.9	46.8	64.7
80 to 100	1,422	326	397	84.3	118.6	52.8
100 to 140	1,371	254	382	54.8	211.4	58.2
140 to 180	586	207	272	23.2	253.9	83.8
180 to 220	293	158	658	-6.5	257.1	94.5
220 to 300	241	161	585	-13.6	175.5	113.2
300 to 380	73	96	576	-13.0	98.1	128.1
380 to 460	46	391	581	-27.8	-10.7	192.5
460 to 520	14	518	731	-15.2	80.3	120.5

Fig. 3. Percentage variation of NC in various size bins for lower height during preheat and stir fry for different activities (a) Breakfast, (b) Lunch, and (c) Dinner. % C (5 min) denotes the percentage change in reading following a 5-minute interval, while % C (10 min) signifies the percentage change after 10 minutes, and so forth.

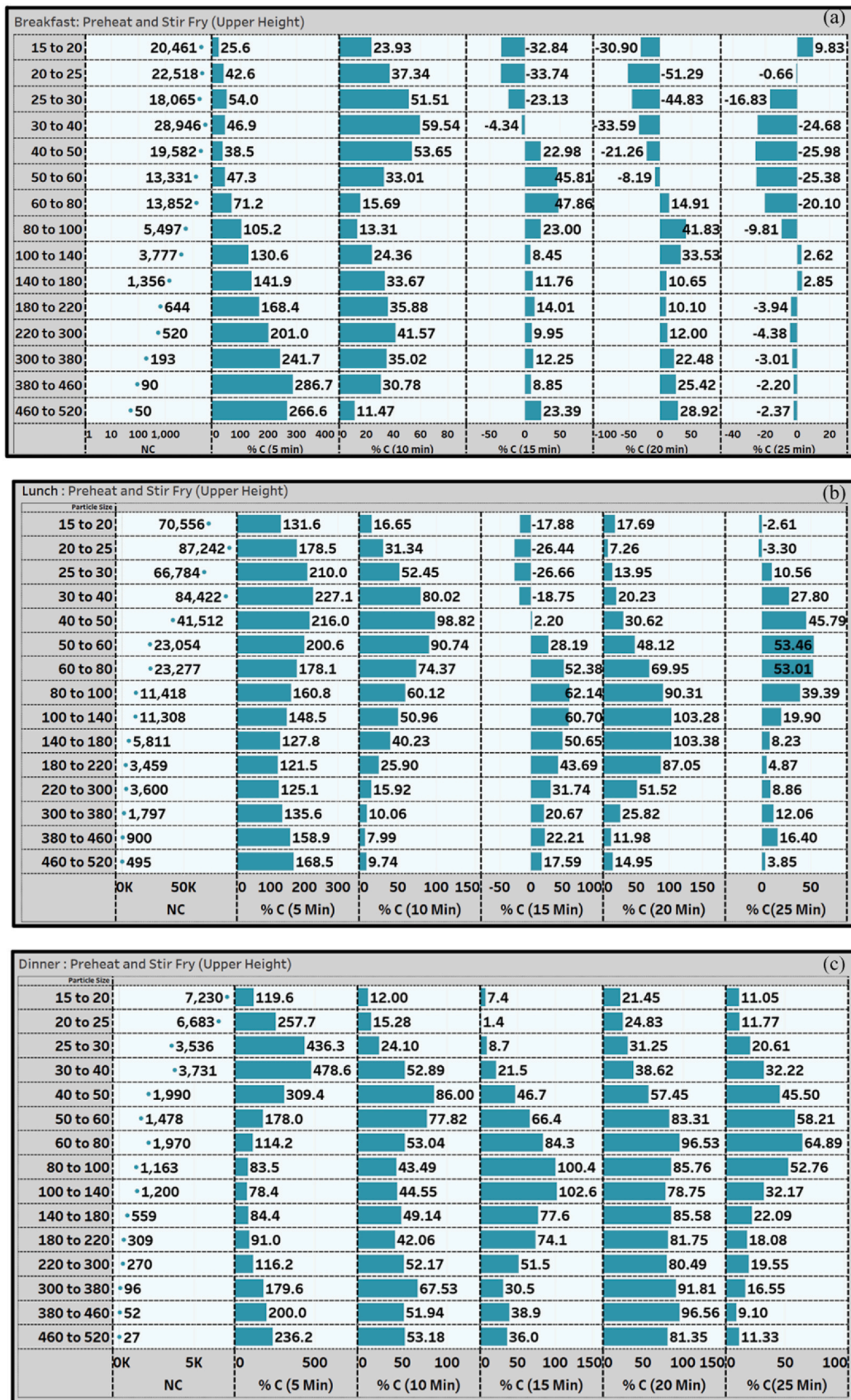


Fig. 4. Percentage variation of NC in various size bins for upper height during preheat and stir fry for different activities (a) Breakfast, (b) Lunch, and (c) Dinner. % C (5 min) denotes the percentage change in reading following a 5-minute interval, while % C (10 min) signifies the percentage change after 10 minutes, and so forth.

**Table 2**  
TNC (number/cm<sup>3</sup>) of UFP emission during different cooking processes and activities.

Activity	Processes	Lower Height				Upper Height			
		Average	SD	Minimum	Maximum	Average	SD	Minimum	Maximum
Breakfast	Preheating	6.3E+05	5.2E+05	4.2E+05	1.2E+06	2.3E+05	1.3E+05	1.6E+05	3.0E+05
	Stir Fry	5.9E+05	3.4E+05	4.4E+04	6.1E+05	3.6E+05	3.0E+05	3.4E+05	3.7E+05
Lunch	Preheating	4.4E+04	3.0E+04	2.5E+04	8.0E+04	1.9E+05	9.3E+04	3.4E+04	2.3E+05
	Stir Fry	3.2E+05	1.7E+05	1.6E+05	3.8E+05	3.1E+05	1.3E+05	2.6E+05	3.7E+05
	Reheat	6.1E+05	6.5E+04	3.5E+05	8.5E+05	3.3E+05	1.2E+04	9.1E+04	3.9E+05
	DeepFry	5.7E+05	4.8E+04	3.5E+05	7.4E+05	4.9E+05	2.9E+05	9.1E+04	3.9E+05
Dinner	Preheating	1.3E+05	8.4E+04	2.0E+04	2.8E+05	1.0E+05	5.8E+04	6.3E+04	1.4E+05
	Stir Fry	3.2E+05	1.8E+05	2.9E+05	3.5E+05	1.9E+05	4.4E+04	1.4E+05	2.7E+05
	Reheat	4.7E+05	2.8E+05	3.1E+05	6.5E+05	4.3E+05	3.3E+04	1.9E+05	7.0E+05
	DeepFry	3.2E+05	1.8E+05	1.5E+05	7.1E+05	4.8E+05	4.2E+04	2.6E+05	8.4E+05

than 300 nm, ultimately leading to elevated PM concentrations at the end of the stir fry process.

After the breakfast activity, there is no cooking process for 60 minutes, and pollutant decay and settlement will occur with mixed ventilation conditions. For the lunch activity after this settlement period of 60 minutes, and after that the interface doors were again closed for lunch activity under controlled ventilation. During the lunch activity in the controlled ventilation, the AER lies between 6.1 and 8.3 h<sup>-1</sup>, as shown in Fig. 6b. The average AER during lunch activity was 3.9 times during controlled ventilation when compared to the breakfast activity. This might be because of the settlement and mixed ventilation period between breakfast and lunch activity, as the chimney keeps working during mixed ventilation conditions. The AER lies between 4.3 and 9.9 h<sup>-1</sup> for the mixed ventilation condition during lunch

activity. The average AER during lunch activity was 1.5 times during mixed ventilation when compared to the breakfast activity. Due to higher AER during the lunch activity compared to the breakfast for controlled ventilation, the concentration of UFP below 100 nm is reduced compared to the breakfast activity. Due to the continuous emissions from the cooking processes, the fine and coarse UFP are still present inside zone 1, and due to chimney suction, increased temperature, and RH, these particles cause higher PM concentrations at upper height.

The AER varies from 4.8–7.9 h<sup>-1</sup> for the dinner activity during controlled ventilation, and the AER varies between –5.1 and 8.8 h<sup>-1</sup> during mixed ventilation. The AER during dinner was 3.3 times during controlled ventilation compared to the breakfast activity during the ventilation. Higher AER during the controlled ventilation in dinner

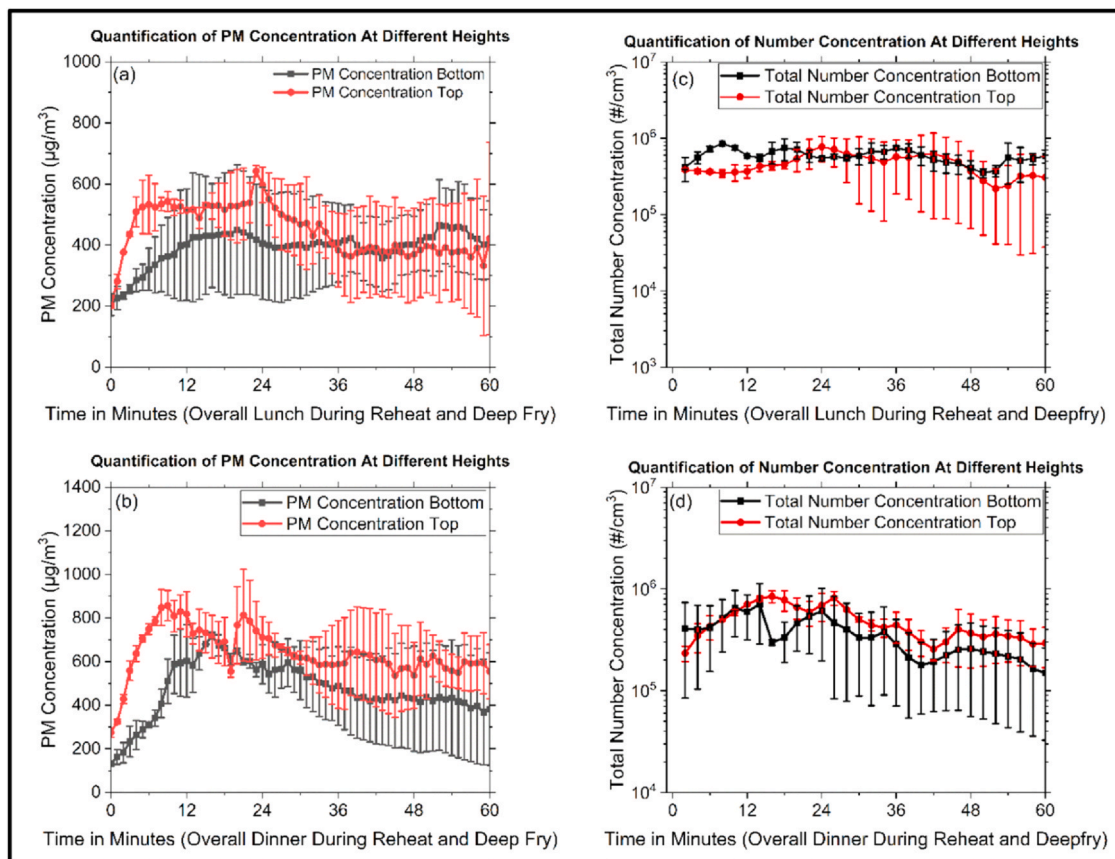


**Fig. 5.** Comparison of (a) PM<sub>2.5</sub> for lunch, (b) PM<sub>2.5</sub> for dinner, (c) TNC for lunch, and (d) TNC for dinner emissions from reheat and deep fry processes during lunch and dinner at different heights.

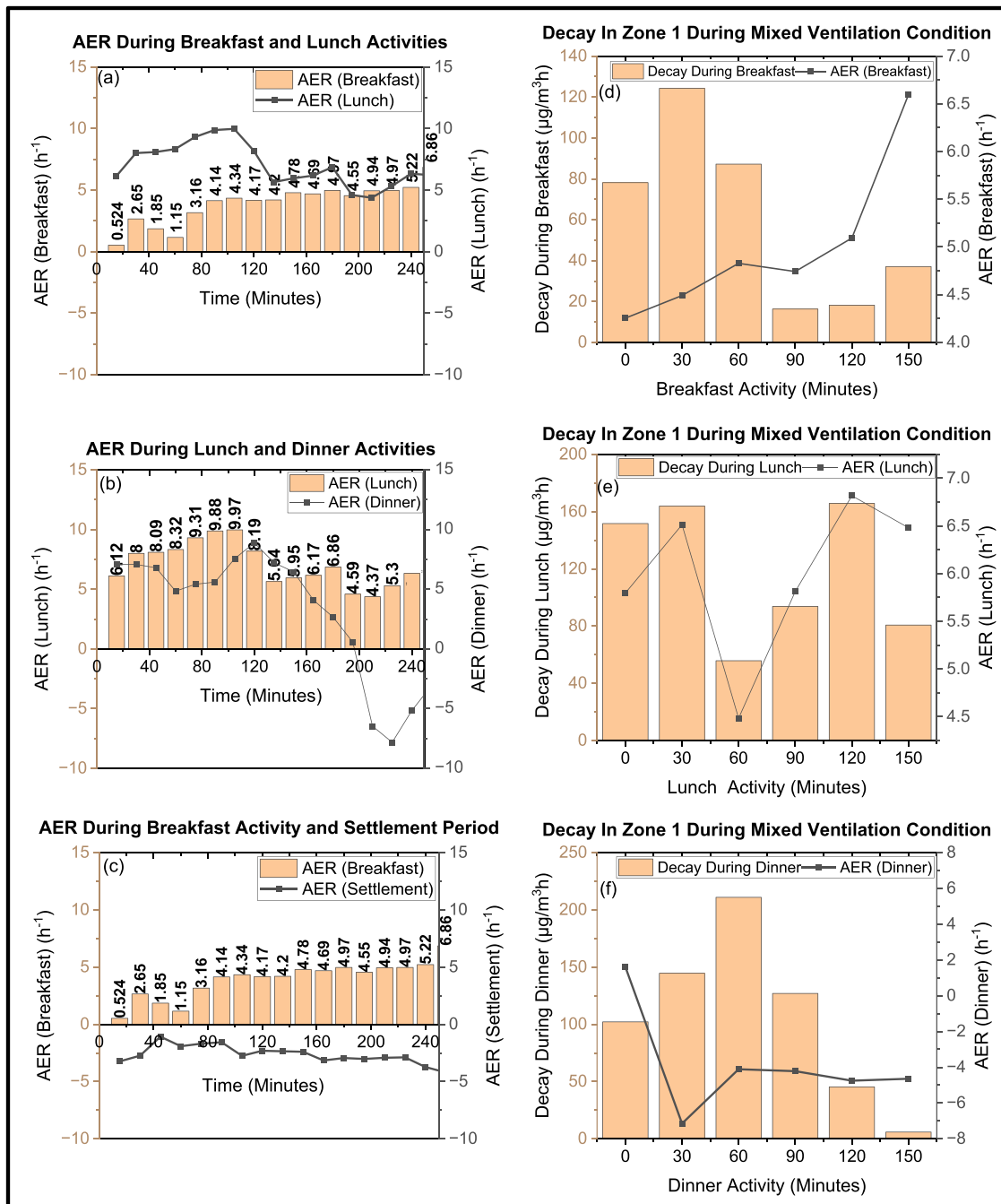


**Fig. 6.** AER variation during (a) Breakfast vs. lunch, (b) Lunch vs. dinner, and (c) Breakfast vs. settlement period. The decay of PM concentration and comparison with AER during (d) breakfast, (e) lunch, and (f) dinner. The zero minutes for d,e, and f show the point where the cooking stove was extinguished.

activity indicates a decrement in UFP compared to breakfast activity. During the dinner activity, particles smaller than 100 nm were prevalent in the preheat phase, similar to the lunch activity. However, due to elevated humidity levels, these particles rapidly grew in size during a short timeframe until the preheat phase was over. As the cooking process continues, there is a subsequent increase in RH. The particle growth becomes particularly pronounced, leading to particles settling down. Consequently, this results in a lesser increase in MC during dinner activity than other activities.

Based on the findings from AER results, the predominant airflow direction is from zone 2 to zone 1 because of the chimney. A chimney creates a natural upward airflow driven by the pressure difference between the inlet and the surrounding atmosphere. The chimney equipped inside zone 1 is a Danish-type ventilation system typically

used in the office building, which involves using a supply fan to introduce outdoor air into the building while simultaneously removing more volume of indoor air from inside using an exhaust fan. The goal is to maintain an equal volume of air entering and leaving zone 1, and two doors connect zone 1 to zone 2. The chimney expelling air to the outside is located on the left side of zone 1, while the chimney introducing air into zone 1 is situated on the right side.

The airflow variation can happen from individual doors connecting the different zones, especially in a variable air volume control system. As a result, doors receiving a higher volume of supplied air may experience a positive internal pressure relative to adjacent doors, causing excess air to flow from one door compared to the other. This arrangement can potentially contribute to spreading the PM and UFP from zone 1 to zone 2, causing an increase in concentration inside zone 2 during

different activities and processes [43]. Ensuring that the extracted airflow matches the supplied airflow for each room is crucial to achieving the desired door pressurization and minimizing this issue. This change of flow between the doors can cause the flow of PM and UFP from zone 1 to zone 2 and cause increased concentrations in zone 2.

### 3.3. Decay rate analysis

#### a) Decay inside the zone 1

Several researchers have conducted experimental and modeling studies to study how pollutants spread out and decrease in enclosed areas with regulated ventilation [3,17,27]. With continuous sampling after the cooking stove is extinguished, it is possible to calculate the post-extinguished PM<sub>2.5</sub> decay rate as well as figure out how efficiently air exchange is happening between zone 1 and zone 2 for the removal of PM<sub>2.5</sub> concentration. Fig. 6d, e, and f represent how the decay varied with AER for breakfast, lunch, and dinner activity, respectively.

During breakfast, lunch, and dinner activity, at lower height sensor, the average decay rate was 64, 126, and 126  $\mu\text{gm}^{-3}\text{h}^{-1}$ , and the average AER during that decay period was 5, 5.9, and  $-3.4\text{h}^{-1}$ , respectively. These results indicate that the decay rate is faster during lunch than during breakfast and dinner activities. The AER was also high during lunch activity, and hence, these overall trends show that the decay rate increases as AER increases inside zone 1, as shown in Fig. 6d, e, and f. The decay rate averaged 101  $\mu\text{gm}^{-3}\text{h}^{-1}$  during breakfast, 129  $\mu\text{gm}^{-3}\text{h}^{-1}$  during lunch, and 132  $\mu\text{gm}^{-3}\text{h}^{-1}$  during dinner activities at the upper height sensor. These results align with those from the lower height sensor, indicating that the decay rate increases with higher AER. The decay rate was faster at upper height compared to lower height.

#### b) Decay from zone 1 to zone 2

The PM<sub>2.5</sub> from zone 1 travels through the interfaces towards zone 2 under controlled and mixed ventilation conditions. Figure 7a and b depict the decay through zone 1 during different activities for controlled ventilation and mixed ventilation systems, respectively. As explained in the study area, zone 2 is equipped with sensors positioned directly along the path of the interface, specifically at pillars 1 and 2. Additionally, four sensors are placed at two positions at distances of 4.5 and 6.5 feet on the end wall of zone 2, at 11 feet from each other, respectively, as shown in Fig. 1.

Fig. 7a, b, c, and d shows that the PM<sub>2.5</sub> varies at different locations inside zone 1 and zone 2 during breakfast, lunch, and breakfast for controlled and mixed ventilation (mechanical + natural). From Fig. 7a, c, we can say that during controlled ventilation (1 hour of closed interface doors), the PM concentration was higher at lower height inside zone 1. This is because the doors are closed, and AER was also less during that time, so the overall average of one shows that the PM concentration was higher at lower height.

Based on the data shown in Fig. 7b and d, it is evident that PM concentrations were higher at upper height during mixed ventilation periods (specifically, when the interface doors were open). This can be attributed to the increased AER resulting from the open doors, causing particles to ascend and accumulate at higher levels over the three-hour average period. Additionally, in zone 2, at Pillar 1, PM concentrations were higher during dinner than during breakfast and lunch activities. This difference can be attributed to the lower AER during controlled ventilation periods observed in Fig. 6a and b during these activities.

The lowest PM concentration is observed during lunch activity when controlled ventilation is in effect at pillar 1. This is due to the higher AER, which efficiently removes emissions from zone 1 to the outside. In a mixed ventilation scenario, PM concentration was minimal during

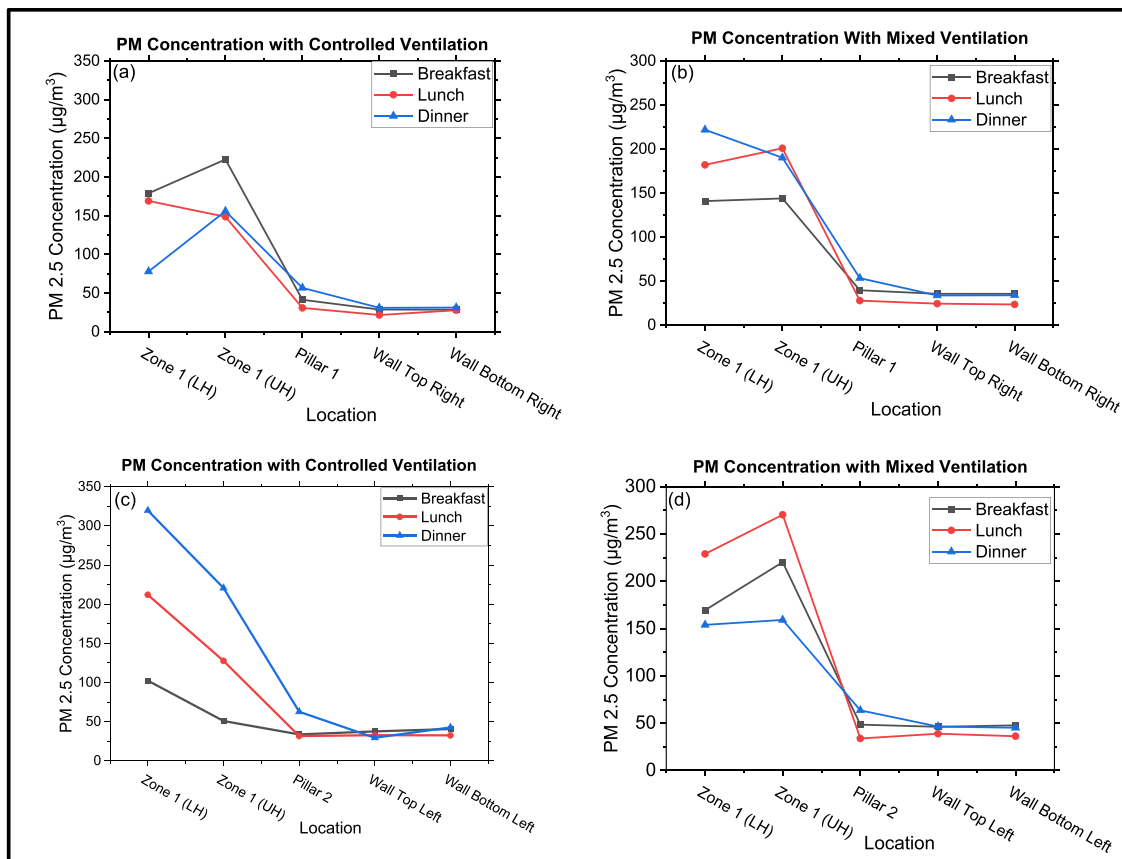


Fig. 7. The variation in PM concentration from zone 1 to zone 2 under (a) controlled ventilation from pillar 1 and (c) controlled ventilation from pillar 2, as well as (b) mixed ventilation from pillar 1 and (d) mixed ventilation from pillar 2.

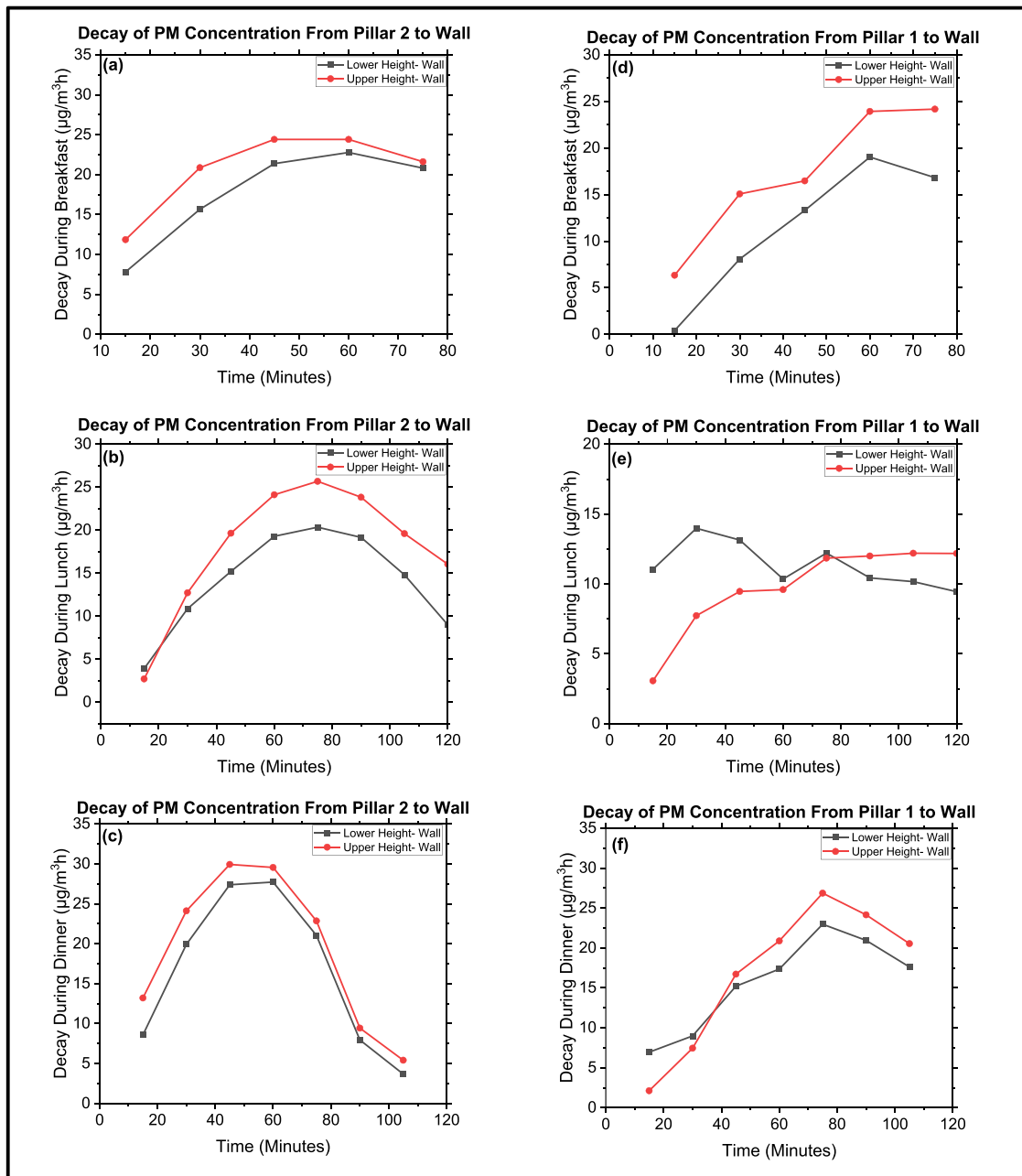


Fig. 8. PM concentration variation in zone 2 from (a) pillar 2 to the wall during breakfast, (b) pillar 2 to the wall during lunch, (c) pillar 2 to the wall during dinner, and (d) pillar 1 to the wall during breakfast, (e) pillar 1 to the wall during lunch, and (f) pillar 1 to the wall during dinner at different heights during breakfast, lunch and dinner activities.

lunch but reached maximum during dinner, primarily because of the fluctuating AER between these two activities. When mixed ventilation was in effect during dinner, the chimney was not in operation. Consequently, air was exchanged for dinner from zone 1 to zone 2, as illustrated in Fig. 6c. This led to a significant rise in PM concentration in zone 2. Similar outcomes were observed for the changes from pillar 2 to the wall, as shown in Fig. 7c and d.

**c) Decay analysis of zone 2**

The analysis done during the mixed ventilation from pillar 1 to the wall is shown in Fig. 8e, f, and g for breakfast, lunch, and dinner activities, respectively, and from pillar 2 to wall is shown in Fig. 8a, b, and c for breakfast, lunch, and dinner activities, respectively.

The varying percentages of PM concentration decay from sensors are found at different locations and times of the day. Pillar 1 exhibited

higher decay rates at the top sensor, with a cumulative 260% higher decay during breakfast and significant differences during lunch and dinner. In contrast, Pillar 2 showed a 22.05% cumulative higher decay rate at the top sensor during breakfast, increasing to 25.26% during lunch and 23.6% during dinner compared to the bottom sensor. These results highlight the influence of ventilation and location on PM concentration decay patterns.

Comparing sensors near pillar 1, the top sensor consistently showed higher decay rates compared to the bottom sensor, with the largest difference observed during breakfast. Similarly, near pillar 2, the top sensor had higher decay rates than the bottom sensor, with the largest difference during lunch. These findings suggest differences in ventilation effectiveness and PM concentration distribution in different scenarios and locations.

### 3.4. Exposure bias analysis and human exposure

In zone 1, the utilization of a Dustrak as a reference monitor was combined with the LCS for calibration purposes. The methodology outlined in the methodology section was implemented to ascertain the bias between the reference monitor and LCS, resulting in the determination of a background concentration of  $28 \mu\text{g}/\text{m}^3$ . Uncalibrated sensor data were compared with Dustrak data, revealing exposure bias. During breakfast, the lowest bias was 0.21, increasing to 0.30 during lunch and 0.22 during dinner, as illustrated in Fig. S10a. More details can be found in S1.5.

Evaluation of individual exposure during different cooking activities revealed that deep-frying results in the highest  $\text{PM}_{2.5}$  intake, accounting for 14% of the total exposure. Following deep-frying, reheating, stir-frying, and preheating activities were associated with elevated  $\text{PM}_{2.5}$  concentrations, as shown in Fig. S10b. In zone 1, male operators had 5% greater  $\text{PM}_{2.5}$  intake than females, primarily due to varying inhalation rates. (more details can be seen in S1.6).

This study provides the latest data on PM and UFP concentration variation during cooking processes and activities in a common dining facility. The main advantage of this study is consistency in the menu; this allows us to have reliable and accurate baseline data. This constancy makes it easier to measure emissions over time and allows for useful comparisons across various cooking activities with cooking processes. Additionally, it permits insightful contrasts across kitchens and dining establishments, acting as a useful benchmarking tool. This study gives a real-time observation of different cooking processes and activities inside the kitchen area, which will accurately represent the personal exposure through inhalation for different kitchen workers worldwide.

### 4. Conclusions

A detailed analysis of the PM and UFP emissions from various cooking activities and cooking processes in a common cooking facility was carried out in this study. Air quality levels in zone 1 (kitchen) as well as the adjoining zone 2 (dining areas) were studied in detail, along with the measurement of temperature and RH for different processes and activities. This study also investigated how there is a change in PM and UFP concentration at different heights in zone 1 and zone 2. It was observed that there is an overall increment of 54%, 186%, and 163% during different activities in  $\text{PM}_{2.5}$  concentration when processes change from preheating to stir fry, preheating to reheating, and stir-fry to deep-fry, respectively. Further, The  $\text{PM}_{2.5}$  concentration exhibits higher values at upper height within zone 1 for different processes and activities, indicating its sensitivity to temperature and RH. The TNC correlates positively with  $\text{PM}_{2.5}$  for certain processes and activities and inversely for others due to increased particle size or diameter during cooking. This can be attributed to the relative importance of UFP, fine particles, and coarser UFP.

Additionally, results provide insights into the effect of mechanical ventilation on the AER and decay rate during controlled (only chimney with closed doors) and mixed (chimney with opened doors) ventilation scenarios inside zone 1. AER was maximum during lunch activity ( $4.3\text{--}9.9 \text{ h}^{-1}$ ) compared to breakfast activity ( $7.8\text{--}6.8 \text{ h}^{-1}$ ) and dinner activity ( $0.55\text{--}7.9 \text{ h}^{-1}$ ) during controlled (less AER) and mixed (more AER) ventilation. The maximum decay rate was also during lunch activity ( $126.18 \mu\text{g m}^{-3} \text{ h}^{-1}$ ), followed by dinner activity ( $126.02 \mu\text{g m}^{-3} \text{ h}^{-1}$ ), and finally, in breakfast activity ( $64 \mu\text{g m}^{-3} \text{ h}^{-1}$ ); these results suggest that the decay rates are correlated with AER. The higher AER during lunch is also a possible reason for lower concentration in zone 2 compared to breakfast and dinner activities. Exposure bias assessments highlight differences between calibrated and uncalibrated sensor data, which is vital for accurate IAQ assessments. Lastly, human exposure analysis emphasizes the impact of cooking methods on  $\text{PM}_{2.5}$  intake, with deep-frying and stir-frying showing higher levels and male

operators generally experiencing relatively higher intake. The insight from these results can help to improve IAQ management in commercial kitchens, guiding ventilation strategies to minimize indoor pollutant exposure during cooking activities and promoting healthier cooking practices. Enhancing the ventilation system using suitable masks and appropriate filtration technology can reduce exposure.

### Funding

T.T. gratefully acknowledges the support from Indian Institute of Technology Goa through the project 2018/TT/SG/006. A.J acknowledges the support of the Ministry of Education, India through the Prime Minister Research Fellowship (PMRF).

### CRediT authorship contribution statement

**Akshat Jain:** Methodology, Investigation, Conceptualization. **Anirudha Ambekar:** Writing – review & editing, Supervision, Project administration, Investigation, Formal analysis. **Thaseem Thajudeen:** Writing – review & editing, Supervision, Resources, Project administration, Funding acquisition, Conceptualization. **Sarath K. Guttikunda:** Writing – review & editing, Resources, Methodology. **Rubal Dhiman:** Writing – original draft, Methodology, Investigation, Formal analysis, Data curation, Conceptualization. **Rajat Sharma:** Writing – original draft, Investigation, Formal analysis, Data curation.

### Declaration of Competing Interest

The authors declare that they have no known competing financial interests or personal relationships that could have appeared to influence the work reported in this paper.

### Appendix A. Supporting information

Supplementary data associated with this article can be found in the online version at [doi:10.1016/j.indenv.2024.100008](https://doi.org/10.1016/j.indenv.2024.100008).

### References

- [1] J. Mu, J. Kang, *Front. Public Heal* 10 (2022) 1–23.
- [2] S. Zheng, H. Shen, G. Shen, Y. Chen, J. Ma, H. Cheng, S. Tao, *Environ. Sci. Ecotechnology* 12 (2022) 100200.
- [3] S. Patel, J. Li, A. Pandey, S. Pervez, R.K. Chakrabarty, P. Biswas, *Environ. Res.* 152 (2017) 59–65.
- [4] K. Slezakova, E. de Oliveira Fernandes, M. do C. Pereira, *Environ. Pollut.* 246 (2019) 885–895.
- [5] D.A. Hapidin, C. Saputra, D.S. Maulana, M.M. Munir, K. Khairurrijal, *Aerosol Air Qual. Res.* 19 (2019) 181–194.
- [6] H. Khreis, J. Johnson, K. Jack, B. Dadashova, E.S. Park, *Int. J. Environ. Res. Public Health* 19 (2022).
- [7] S.C.C. Lung, T.T. Hien, M.O.L. Cambaliza, O.M.T. Hlaing, N.T.K. Oanh, M.T. Latif, P. Lestari, A. Salam, S.Y. Lee, W.C.V. Wang, M.C.M. Tsou, T. Cong-Thanh, M.T. Cruz, K. Tantrakarnapa, M. Othman, S. Roy, T.N. Dang, D. Agustian, *Int. J. Environ. Res. Public Health* 19 (2022).
- [8] J. Zhang, Z. Zhou, C. Wang, K. Xue, Y. Liu, M. Fang, J. Zuo, Y. Sheng, *IOP Conf. Ser. Mater. Sci. Eng.* 585 (2019).
- [9] G. Chinazzo, R.K. Andersen, E. Azar, V.M. Barthelmes, C. Becchio, L. Belussi, C. Berger, S. Carlucci, S.P. Corgnati, S. Crosby, L. Danza, L. de Castro, M. Favero, S. Gauthier, R.T. Hellwig, Q. Jin, J. Kim, M. Sarey Khanie, D. Khowalyg, C. Lingua, A. Luna-Navarro, A. Mahdavi, C. Miller, I. Mino-Rodriguez, I. Pigliautile, A.L. Pisello, R.F. Rupp, A.M. Sadick, F. Salamone, M. Schweiker, M. Sydicus, G. Spigiantini, N.G. Vasquez, D. Vakalis, M. Vellei, S. Wei, *Build. Environ.* 226 (2022) 109719.
- [10] B.N. Young, M.L. Clark, S. Rajkumar, M.L. Benka-Coker, A. Bachand, R.D. Brook, T. L. Nelson, J. Volckens, S.J. Reynolds, C. L'Orange, N. Good, K. Koehler, S. Africano, A.B. Osorto Pinel, J.L. Peel, *Exposure to Household Air Pollution from Biomass Cookstoves and Blood Pressure among Women in Rural Honduras: A Cross-Sectional Study*, 2019.
- [11] X. Huang, D. Han, J. Cheng, X. Chen, Y. Zhou, H. Liao, W. Dong, C. Yuan, *Environ. Sci. Pollut. Res.* 27 (2020) 490–499.
- [12] Y. Zhao, B. Zhao, *Build. Simul.* 11 (2018) 977–995.
- [13] M.K. Sidhu, K. Ravindra, S. Mor, S. John, *Sci. Total Environ.* 586 (2017) 419–429.
- [14] A. Dutta, H. Chattopadhyay, *J. Therm. Biol.* 96 (2021).
- [15] D. Sharma, S. Jain, *Environ. Int.* 123 (2019) 240–255.

- [16] M.T. Baeza\_Romero, M.R. Dudzinska, M. Amouei Torkmahalleh, N. Barros, A.M. Coggins, D.G. Ruzgar, I. Kildsgaard, M. Naseri, L. Rong, J. Saffell, A.M. Scutaru, A. Staszowska, *Indoor Air* 32 (2022) 1–16.
- [17] J. Xiang, J. Hao, E. Austin, J. Shirai, E. Seto, *Build. Environ.* 201 (2021) 108002.
- [18] M.P. Wan, C.L. Wu, G.N. Sze To, T.C. Chan, C.Y.H. Chao, *Atmos. Environ.* 45 (2011) 6141–6148.
- [19] C. He, L. Morawska, D. Gilbert, *Atmos. Environ.* 39 (2005) 3891–3899.
- [20] Y. Deepthi, S.M. Shiva Nagendra, S.N. Gummadi, *Sci. Total Environ.* 650 (2019) 616–625.
- [21] P. Desouza, R. Kahn, T. Stockman, W. Obermann, B. Crawford, A. Wang, J. Crooks, J. Li, P. Kinney, *Atmos. Meas. Tech.* 15 (2022) 6309–6328.
- [22] J.V. Jagatha, A. Klausnitzer, M. Chacón-Mateos, B. Laquai, E. Nieuwkoop, P. van der Mark, U. Vogt, C. Schneider, *Sensors* 21 (2021).
- [23] D. Bousiotis, L.N.S. Alconcel, D.C.S. Beddows, R.M. Harrison, F.D. Pope, *Environ. Int.* 174 (2023) 107907.
- [24] R. Tang, C. Pfrang, *Environ. Sci. Atmos.* 3 (2023) 537–551.
- [25] B. Alfano, L. Barretta, A. Del Giudice, S. De Vito, G. Di Francia, E. Esposito, F. Formisano, E. Massera, M.L. Miglietta, T. Polichetti, *Sensors* 21 (2021).
- [26] X. Gao, W. Gao, X. Sun, W. Jiang, Z. Wang, W. Li, *Atmosphere* 11 (2020).
- [27] D. Rim, L. Wallace, S. Nabinger, A. Persily, *Sci. Total Environ.* 432 (2012) 350–356.
- [28] S.C. Lee, W.M. Li, L. Yin Chan, *Sci. Total Environ.* 279 (2001) 181–193.
- [29] M.S. Breen, B.D. Schultz, M.D. Sohn, T. Long, J. Langstaff, R. Williams, K. Isaacs, Q.Y. Meng, C. Stallings, L. Smith, *J. Expo. Sci. Environ. Epidemiol.* 24 (2014) 555–563.
- [30] A.C.K. Lai, Y.W. Ho, *Build. Environ.* 43 (2008) 871–876.
- [31] M.S. Hossain, W. Che, H.C. Frey, A.K.H. Lau, *Build. Environ.* 206 (2021) 108351.
- [32] R. Suresh, D. Sharma, P. Arora, A. Sharma, R.C. Pal, *Aerosol Sci. Eng.* 6 (2022) 400–413.
- [33] D.E. Schraufnagel, *Exp. Mol. Med.* 52 (2020) 311–317.
- [34] P. Kumar, L. Morawska, *City Environ. Interact.* 4 (2019) 100033.
- [35] A. Masic, D. Bibic, B. Pikula, A. Blazevic, J. Huremovic, S. Zero, *Atmos. Meas. Tech.* 13 (2020) 6427–6443.
- [36] C. McFarlane, G. Raheja, C. Malings, E.K.E. Appoh, A.F. Hughes, D.M. Westervelt, *ACS Earth Sp. Chem.* 5 (2021) 2268–2279.
- [37] A. Standard, *Ashrae Stand* (2009) 24–25.
- [38] Q. Zhang, R.H. Gangupomu, D. Ramirez, Y. Zhu, *Int. J. Environ. Res. Public Health* 7 (2010) 1744–1759.
- [39] Risk Assess USEPA, Forum, D.C. Washington, 57 (1992) 22888–22938.
- [40] A. Mehadi, H. Moosmüller, D.E. Campbell, W. Ham, D. Schweizer, L. Tarnay, J. Hunter, *J. Air Waste Manag. Assoc.* 70 (2020) 158–179.
- [41] T. Sayahi, A. Butterfield, K.E. Kelly, *Environ. Pollut.* 245 (2019) 932–940.
- [42] C.Y. Ng, X.F. Leong, N. Masbah, S.K. Adam, Y. Kamisah, K. Jaarin, *Vascul. Pharmacol.* 61 (2014) 1–9.
- [43] A. Afshari, G. Hultmark, P.V. Nielsen, A. Maccarini, *Front. Built Environ.* 7 (2021) 1–10.